

Nicos Makris · Michalis F. Vassiliou

# Sizing the slenderness of free-standing rocking columns to withstand earthquake shaking

Received: 24 October 2011 / Accepted: 8 May 2012  
© Springer-Verlag 2012

**Abstract** This paper investigates the problem of sizing the width of tall free-standing columns with a given height which are intended to rock, yet shall remain stable during the maximum expected earthquake shaking. The motivation for this study is the emerging seismic design concept of allowing tall rigid structures to uplift and rock in order to limit base moments and shears. The paper first discusses the mathematical characterization of pulse-like ground motions and the dimensionless products that govern the dynamics of the rocking response of a free-standing block and subsequently, using basic principles of dynamics, derives a closed-form expression that offers the minimum design slenderness that is sufficient for a free-standing column with a given size to survive a pulse-like motion with known acceleration amplitude and duration.

**Keywords** Rocking · Stability · Limit state analysis · Earthquake engineering · Seismic design

## 1 Introduction

Reconnaissance reports following strong earthquakes include the uplift, rocking, or overturning of a variety of slender structures such as tombstones, electrical equipment, retaining walls, liquid storage tanks, and rigid building structures. The need to understand and predict these failures in association with the temptation to estimate levels of ground motions by examining whether slender structures have overturned or survived historic earthquakes has motivated a number of studies on the rocking response of rigid blocks (Milne [1], Housner [2], Yim et al. [3], Spanos and Koh [4], Hogan [5], Shenton [6], Shi et al. [7], Makris and Roussos [8], Zhang and Makris [9] among others, and references reported therein).

Early studies on the rocking response of a rigid block supported on a base undergoing horizontal motion were presented by Housner [2]. In that study, the base acceleration was represented by a rectangular or a half-sine pulse, and expressions were derived for the minimum acceleration amplitude required to overturn the block. Although Housner's pulses are not physically realizable (finite ground velocity at the expiration of the pulse) and his solution for the minimum overturning acceleration under a half-sine pulse is unconservative (Shi et al. [7]; Makris and Roussos [8, 10]), his pioneering work uncovered a size-frequency scale effect that explained (a) why the larger of two geometrically similar blocks can survive the excitation that will topple the smaller block and (b) why out of two same acceleration-amplitude pulses the one with the longer duration is more capable of inducing overturning.

---

N. Makris (✉) · M. F. Vassiliou  
Department of Civil Engineering, University of Patras, 26500 Patras, Greece  
E-mail: nmakris@upatras.gr

*Present Address:*  
M. F. Vassiliou  
Institute of Structural Engineering, ETH Zurich, 8093 Zurich, Switzerland  
E-mail: mfvassiliou@gmail.com



**Fig. 1** *Left* view of the South Rangitikei bridge in New Zealand. The piers are allowed to lift up to 13 cm while rocking along the transverse direction of the bridge. *Right* close view of the stepping pier at the location where uplift happens

Following Housner's pioneering work, several studies from other investigators (Aslam et al. [11], Yim et al. [3], Spanos and Koh [4], Tso and Wong [12,13], Psycharis [14], Shenton [6], Makris and Roussos [8,10], Zhang and Makris [9], Makris and Konstantinidis [15], Apostolou et al. [16], Anastassopoulos et al. [17] among others) showed that the uplifting and rocking of tall-slender structures has beneficial effects on their seismic resistance.

The beneficial effects that derive from uplifting and rocking have been implemented at present to a limited number of bridge piers, such as the Rangitikei bridge in New Zealand (see Fig. 1) (Beck and Skinner [18]), the Rion-Antirion bridge in Greece (Pecker [19]), and the Rio-Vista bridge in California (Yashinsty and Karshenas [20]).

The main challenge in designing rocking structures in order to limit overturning moments and base shears is that the restoring moment of a rocking structure decreases as rotation increases and eventually becomes unstable when the rotation exceeds the slenderness,  $\alpha$ , of the free-standing structure. Accordingly, when sizing a rocking structure, it has to be slender enough to undergo rocking; while, it has to be wide enough in order to remain stable, given the seismic hazard of the area that it belongs to. The scope of this paper is to examine what shall be the minimum design slenderness (maximum allowable ratio of height over base) of a rocking structure with a given size to survive strong ground shaking that may happen in a given area.

Recently, Gelagoti et al. [21] have investigated the potential benefits of the uplifting mechanism of the foundation of frame structures and proposed a simplified procedure by reverting to the elastic response spectrum in order to estimate the minimum acceptable width of the foundation that will ensure stability. In contrast to the simplified procedure proposed in [21], in this study we deal strictly with the rocking mechanism of a free-standing slender block (without leaning to the elastic oscillator and its elastic response spectrum), and by using basic principles of dynamics, we derive a closed-form expression that offers the minimum design slenderness that is sufficient for the block to survive a strong pulse-like excitation that is characterized with an acceleration amplitude  $a_p$  and a duration  $T_p$ .

While the early work of Yim et al. [3] used artificially generated white-noise-type motions and the work of Spanos and Koh [4], Hogan [5], and Tso and Wong [12,13] used long-duration harmonic motions, this paper is redirected to pulse-type motions, which are found to be good representations of near-source ground motions (Bertero et al. [22], Campillo et al. [23], Iwan and Chen [24], Hall et al. [25], Heaton et al. [26], Makris [27], Makris and Roussos [8], Mavroeidis and Papageorgiou [28], Vassiliou and Makris [29]). Herein, this study builds on past work of the senior author to investigate the overturning potential of pulse-like ground motions [8–10,30]. Given that the scope of the paper is to offer the minimum design slenderness, the study reverts to the rectangular pulse initially used by Housner—an acceleration pulse that while not physically realizable on the ground allows for the derivation of an analytical solution which also meets the need of being conservative.

## 2 Review of the rocking response of a rigid block

With reference to Fig. 2 and assuming that the coefficient of friction is large enough so that there is no sliding, the equation of motion of a free-standing block with size  $R = \sqrt{h^2 + b^2}$  and slenderness  $\alpha = a \tan(b/h)$

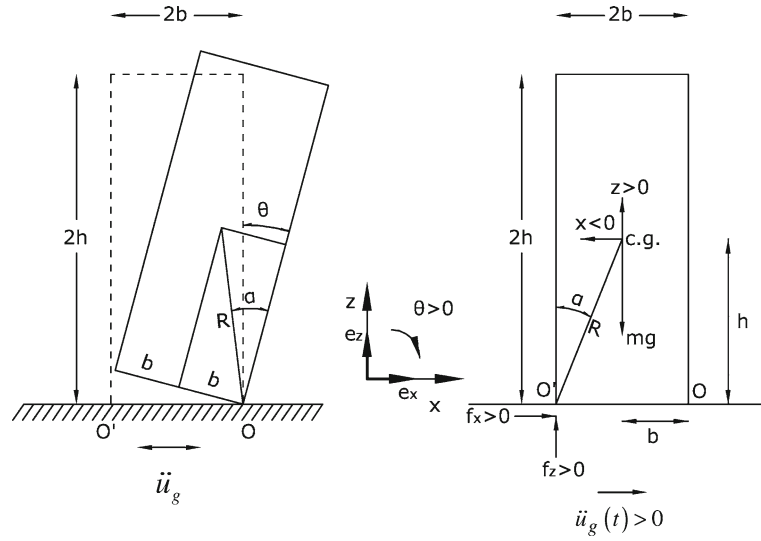


**Fig. 2** *Left* geometric characteristics of the model considered. *Right* free-body diagram of a free-standing block at the instant that it enters rocking motion

subjected to a horizontal ground acceleration  $\ddot{u}_g(t)$  when rocking around  $O$  and  $O'$ , respectively, is (Yim et al. [3], Makris and Roussos [8], Zhang and Makris [9] among others)

$$I_o \ddot{\theta}(t) + mgR \sin[-\alpha - \theta(t)] = -m\ddot{u}_g(t) R \cos[-\alpha - \theta(t)], \quad \theta(t) < 0 \quad (1)$$

$$I_o \ddot{\theta}(t) + mgR \sin[\alpha - \theta(t)] = -m\ddot{u}_g(t) R \cos[\alpha - \theta(t)], \quad \theta(t) > 0 \quad (2)$$

In order for rocking motion to be initiated,  $\ddot{u}_g(t) > g \tan \alpha$  at some time of its history. For an ancient column, the coefficient of friction along a marble or a limestone interface is  $\mu > 0.7$ —a value that is much larger than the uplift acceleration  $g \tan \alpha$ . Accordingly, ancient stone columns enter rocking motion—not sliding. During impact, high accelerations develop, and in this case, some minor sliding may take place. Nevertheless, larger columns that are of interest in this study overturn without impact (Zhang and Makris [9]); consequently, the possible minor sliding during impact is immaterial to this analysis.

For rectangular blocks,  $I_o = (4/3) m R^2$ , and the above equations can be expressed in the compact form

$$\ddot{\theta}(t) = -p^2 \left\{ \sin[\alpha \operatorname{sgn}(\theta(t)) - \theta(t)] + \frac{\ddot{u}_g}{g} \cos[\alpha \operatorname{sgn}(\theta(t)) - \theta(t)] \right\} \quad (3)$$

The oscillation frequency of a rigid block under free vibration is not constant, because it strongly depends on the vibration amplitude (Housner [2]). Nevertheless, the quantity  $p = \sqrt{\frac{3g}{4R}}$  is a measure of the dynamic characteristics of the block. For the  $7.5 \times 1.8$  m free-standing column of the Temple of Apollo in Corinth,  $p = 1.4$  rad/s, and for a household brick,  $p \approx 8$  rad/s.

Figure 3 shows the moment–rotation relationship during the rocking motion of a free-standing block. The system has infinite stiffness until the magnitude of the applied moment reaches the value  $mgR \sin \alpha$ , and once the block is rocking, its restoring force decreases monotonically, reaching zero when  $\theta = \alpha$ . This negative stiffness, which is inherent in rocking systems, is most attractive in earthquake engineering in terms of keeping base shears and moments low (Makris and Konstantinidis [15]), provided that the rocking block remains stable, thus the need for a formulae that will offer a safe design value for its slenderness.

During the oscillatory rocking motion, the moment–rotation curve follows the curve shown in Fig. 3 without enclosing any area. Energy is lost only during impact, when the angle of rotation reverses. The ratio of kinetic energy after and before the impact is

$$r = \frac{\dot{\theta}_2^2}{\dot{\theta}_1^2} \quad (4)$$

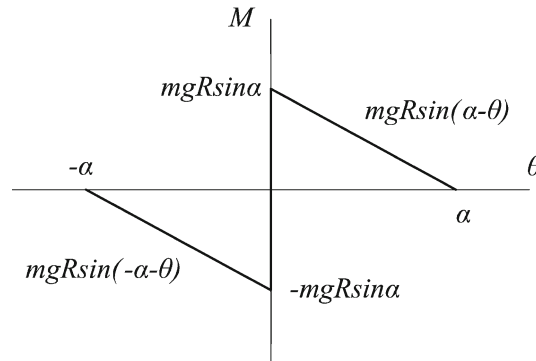


**Fig. 3** Moment–rotation diagram of a rocking object with slenderness  $\alpha$  and size  $R$

which means that the angular velocity after the impact is only  $\sqrt{r}$  times the velocity before the impact. Conservation of angular momentum just before and right after the impact gives:

$$r = \left[ 1 - \frac{3}{2} \sin^2 \alpha \right]^2 \quad (5)$$

The value of the coefficient of restitution given by (5) is the maximum value of  $r$ , under which a block with slenderness  $\alpha$  will undergo rocking motion. Consequently, in order to observe rocking motion, the impact has to be inelastic. The less slender a block is (larger  $\alpha$ ), the more plastic the impact is, and for the value of  $\alpha = \sin^{-1} \sqrt{2/3} = 54.73^\circ$ , the impact is perfectly plastic. During the rocking motion of slender blocks, if additional energy is lost due to the inelastic behavior at the instant of impact, the value of the true coefficient of restitution  $r$  will be less than the one computed from Eq. (5).

### 3 Time scale and length scale of pulse-like ground motions

The relative simple form, yet destructive potential of near-source ground motions has motivated the development of various closed-form expressions that approximate their leading kinematic characteristics. The early work of Veletsos et al. [31] was followed by the papers of Hall et al. [25], Heaton et al. [26], Makris [27], Makris and Chang [32], Alavi and Krawinkler [33], and more recently by Mavroeidis and Papageorgiou [28]. Some of the proposed pulses are physically realizable motions with zero final ground velocity and finite accelerations, whereas some other idealizations violate one or both of the above requirements. Physically realizable pulses can adequately describe the impulsive character of near-fault ground motions both qualitatively and quantitatively. The input parameters of the model have an unambiguous physical meaning. The minimum number of parameters is two, which are either the acceleration amplitude,  $a_p$ , and duration,  $T_p$ , or the velocity amplitude,  $v_p$ , and duration,  $T_p$  (Makris [27], Makris and Chang [32]). The more sophisticated model of Mavroeidis and Papageorgiou [28] involves four parameters, which are the pulse period, the pulse amplitude, and as the number and phase of half cycles, and was found to describe a large set of velocity pulses generated due to forward directivity or permanent translation effect. Recently, Vassiliou and Makris [29] used the Mavroeidis and Papageorgiou model [28] in association with wavelet analysis to develop a mathematically formal and objective procedure to extract the time scale and length scale of strong ground motions.

The pulse period,  $T_p$ , of the most energetic pulse of strong ground motions is strongly correlated with the moment magnitude,  $M_w$ , of the event. For a given moment magnitude, the duration of pulses produced by strike-slip faults is on average larger than the duration of pulses generated by reverse faults [28]. Assuming that the time scale  $T_p$  is independent of the source–station distance, for stations located within  $\sim 10$  km from the causative fault, the pulse period and moment magnitude are related through the following empirical relationship, which also satisfies a self-similarity condition [33,34]:

$$\ln T_p = -2.9 + 0.5M_w \quad (6)$$

Furthermore, seismological data indicate that the amplitude of the velocity pulses recorded within a distance of 7 km from the causative fault varies from 60 to 120 cm/s. This observation is in good agreement with the typical slip velocity value of 90 cm/s frequently considered by seismologists (Brune [35], Aki [36]).

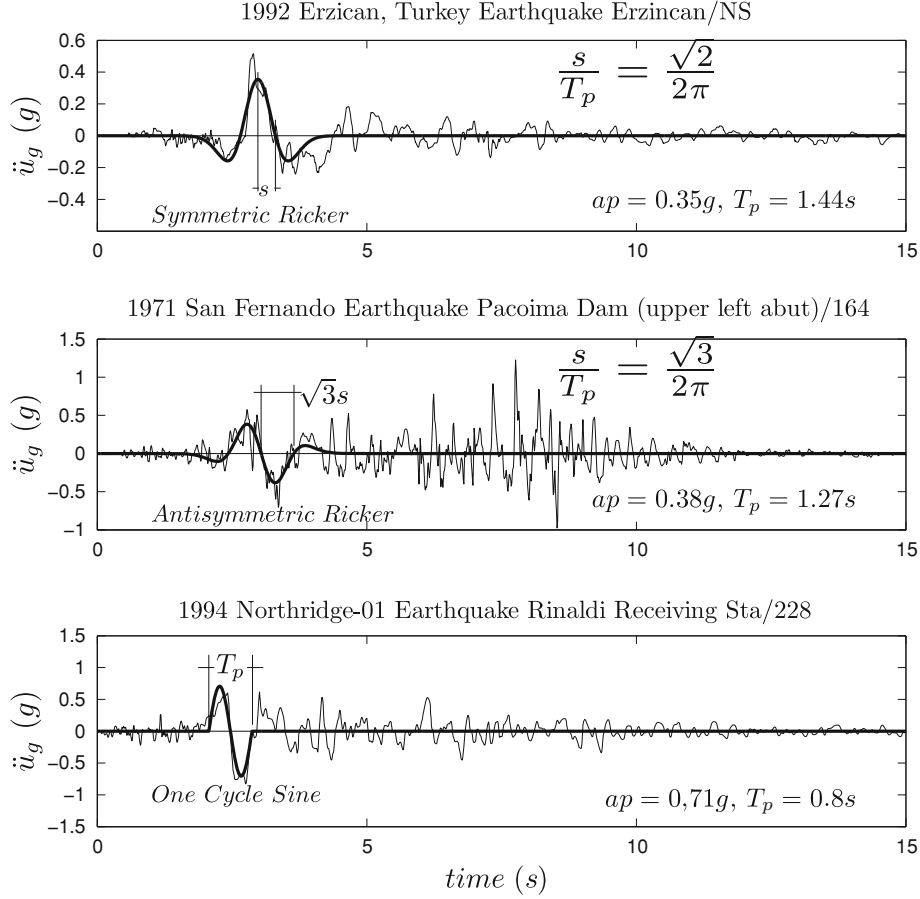


**Fig. 4** Acceleration time histories recorded during the (top) 1992 Erzincan, Turkey, earthquake together with a symmetric Ricker wavelet; (center) 1971 San Fernando earthquake—fault normal component of the Pacoima Dam record together with an antisymmetric Ricker wavelet; and (bottom) 1994 Northridge earthquake—228 Rinaldi station together with a one-cycle sine pulse

The current established methodologies for estimating the pulse characteristics of a wide class of records are of unique value since the product,  $a_p T_p^2 = L_p$ , is a characteristic length scale of the ground excitation and is a measure of the persistence of the most energetic pulse to generate inelastic deformations (Makris and Black [37]). It is emphasized that the persistence of the pulse is a different characteristic than the strength of the pulse, which is measured with the peak pulse acceleration. The reader may recall that among two pulses with different acceleration amplitude (say  $a_{p1} > a_{p2}$ ) and different pulse duration (say  $T_{p1} < T_{p2}$ ), the inelastic deformation does not scale with the peak pulse acceleration (most intense pulse) but with the stronger length scale (larger  $a_p T_p^2 =$  most persistent pulse), Makris and Black [37, 38], Karavassilis et al. [39].

The heavy line in Fig. 4 (top) that approximates the long-period acceleration pulse of the NS component of the 1992 Erzincan, Turkey, record is a scaled expression of the second derivative of the Gaussian distribution,  $e^{-t^2}$ , known in the seismology literature as the symmetric Ricker wavelet (Ricker [40, 41]) and widely referred to as the “Mexican Hat” wavelet (Addison [42])

$$\ddot{u}_g(t) = a_p \left( 1 - \frac{2\pi^2 t^2}{T_p^2} \right) e^{-\frac{1}{2} \frac{2\pi^2 t^2}{T_p^2}} \quad (7)$$

The value of  $T_p = \frac{2\pi}{\omega_p}$  is the period that maximizes the Fourier spectrum of the Symmetric Ricker Wavelet.

Similarly, the heavy line in Fig. 4 (center) which approximates the long-period acceleration pulse of the Pacoima Dam motion recorded during the February 9, 1971, San Fernando, California, earthquake is a scaled expression of the third derivative of the Gaussian distribution  $e^{-t^2}$ . Again, in Eq. (8), the value of  $T_p = \frac{2\pi}{\omega_p}$  is the period that maximizes the Fourier spectrum of the antisymmetric Ricker wavelet.

$$\ddot{u}_g(t) = \frac{a_p}{\beta} \left( \frac{4\pi^2 t^2}{3T_p^2} - 3 \right) \frac{2\pi t}{\sqrt{3}T_p} e^{-\frac{1}{2} \frac{4\pi^2 t^2}{3T_p^2}} \quad (8)$$

in which  $\beta$  is a factor equal to 1.38 that enforces the above function to have a maximum  $= a_p$ .

The choice of the specific functional expression to approximate the main pulse of pulse-type ground motions has limited significance in this work. In the past, simple trigonometric pulses have been used by the senior author (Makris [27], Makris and Chang [32], Makris and Black [37,38]) to extract the time scale and length scale of pulse-type ground motions. For instance, the heavy line in Fig. 4(bottom) which approximates the strong coherent acceleration pulse of the 228 component at the Rinaldi receiving station of the 1994 Northridge earthquake is a one-sine acceleration pulse

$$\ddot{u}_g(t) = a_p \sin(\omega_p t), \quad 0 < t < T_p \quad (9)$$

A mathematically rigorous and easily reproducible methodology based on wavelet analysis to construct the best matching wavelet on a given record (signal) has been recently proposed by Vassiliou and Makris [29].

#### 4 Overturning spectra: self-similar response

Consider a free-standing rigid block subjected to an acceleration pulse (like those shown in Fig. 4) with acceleration amplitude  $a_p$  and pulse duration  $T_p = \frac{2\pi}{\omega_p}$ . From Eq. (3), it results that the response of a rocking free-standing block subjected to an acceleration pulse is a function of five variables

$$\theta(t) = f(p, \alpha, g, a_p, \omega_p) \quad (10)$$

The six (6) variables appearing in Eq. (10),  $\theta \doteq []$ ,  $a_p \doteq [L][T]^{-2}$ ,  $\omega_p \doteq [T]^{-1}$ ,  $p \doteq [T]^{-1}$ ,  $\alpha \doteq []$ ,  $g \doteq [L][T]^{-2}$  involve only two reference dimensions: those of length [L] and time [T]. According to Buckingham's  $\Pi$ -theorem, the number of dimensionless products with which the problem can be completely described is equal to [number of variables in Eq. (10)=6]—[number of reference dimensions=2]. Herein, we select as repeating variables the characteristics of the pulse excitation,  $a_p$  and  $\omega_p$ . The four independent  $\Pi$ -terms are

$$\Pi_\theta = \theta \quad (11)$$

$$\Pi_\omega = \frac{\omega_p}{p} \quad (12)$$

$$\Pi_\alpha = \tan(\alpha) \quad (13)$$

$$\Pi_g = \frac{a_p}{g} \quad (14)$$

With the four dimensionless  $\Pi$ -Terms established, Eq. (10) reduces to

$$\theta(t) = \varphi \left( \frac{\omega_p}{p}, \tan \alpha, \frac{a_p}{g} \right) \quad (15)$$

The rocking response of a rigid block when subjected to a horizontal base acceleration,  $\ddot{u}_g(t)$  is computed by solving equation (3) in association with the minimum energy loss expression given by Eq. (5), which takes place at every impact. The solution of the nonlinear differential equation given by (3) is computed numerically by means of a state-space formulation. The state vector of the system shown in Fig. 2(left) is merely

$$\mathbf{y}(\mathbf{t}) = \begin{bmatrix} \theta(t) \\ \dot{\theta}(t) \end{bmatrix} \quad (16)$$

and the time-derivative vector  $\mathbf{f}(\mathbf{t}) = \dot{\mathbf{y}}(\mathbf{t})$  is

$$\dot{\mathbf{y}}(\mathbf{t}) = \begin{bmatrix} \dot{\theta}(t) \\ -p^2 [\sin[\alpha \text{sgn}[\theta(t)] - \theta(t)] + \frac{\ddot{u}_g(t)}{g} \cos[\alpha \text{sgn}[\theta(t)] - \theta(t)] \end{bmatrix} \quad (17)$$

The numerical integration of (17) is performed with standard ordinary differential equations (ODE) solvers available in MATLAB, The Mathworks [43].

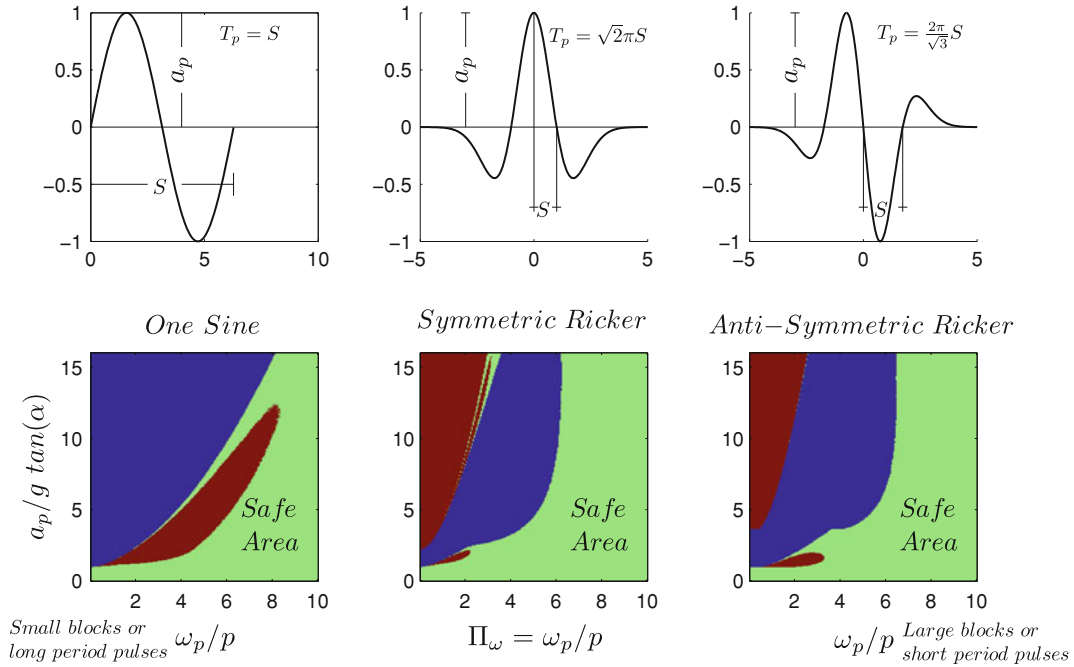


**Fig. 5** Overturning acceleration spectra of a free-standing block with slenderness  $\alpha = 14^\circ$  subjected to a one-sine acceleration pulse (left), a symmetric Ricker wavelet (center), and an antisymmetric Ricker wavelet (right)

Figure 5 shows the overturning acceleration spectrum of a rigid block with slenderness  $\alpha = 14^\circ$  ( $\tan \alpha = 0.25$ ) due to a one-sine acceleration pulse (left), a symmetric Ricker wavelet (center), and an antisymmetric Ricker wavelet (right). Figure 5 indicates that as  $\Pi_\omega = \frac{\omega_p}{p}$  increases, the acceleration needed to overturn the object becomes appreciably larger than the one needed to uplift it.

The light gray (green in the colored version) area in all three bottom plots corresponds to stability (no overturning). Note that all three plots show that there are safe areas above the minimum overturning acceleration—a behavior that results from the strong nonlinear nature of the problem. Most important is that as the ratio  $\Pi_\omega = \frac{\omega_p}{p}$  increases (shorter duration pulses or larger blocks), the minimum overturning acceleration needed to overturn the block increases appreciably. This size-frequency effect illustrated in Fig. 5 shows that a block with a given slenderness can survive strong shaking, provided that it is large enough. What is of interest in this study is to address the other useful design question: What is the minimum allowable slenderness of a free-standing block to remain standing given its size and the acceleration amplitude and duration of the excitation pulse?

## 5 Selection of minimum slenderness (aspect ratio) given a design acceleration pulse

The problem to be addressed is what shall be the minimum allowable slenderness,  $\alpha$ , of a free-standing block with a given frequency parameter,  $p = \sqrt{\frac{3g}{4R}}$  (given size), that can survive the maximum expected ground motion with a strong coherent component that is characterized with an acceleration pulse with amplitude  $a_p$  and duration  $T_p$ .

### 5.1 Approach with dimensional and physical arguments

The solution to the problem addressed above can be approached with the use of the dimensionless products given by Eqs. (12)–(14) in association with the information from static analysis—for a long-duration (constant) acceleration pulse with amplitude  $a_p$ , the overturning acceleration is  $a_p = g \tan \alpha$ . Accordingly, after replacing the dimensionless term  $\Pi_\omega = \frac{\omega_p}{p}$  with  $pT_p$ , the minimum slenderness  $\alpha$  that ensures stability of a free-standing block with size  $R$  subjected to a pulse with amplitude  $a_p$  and duration  $T_p$  is

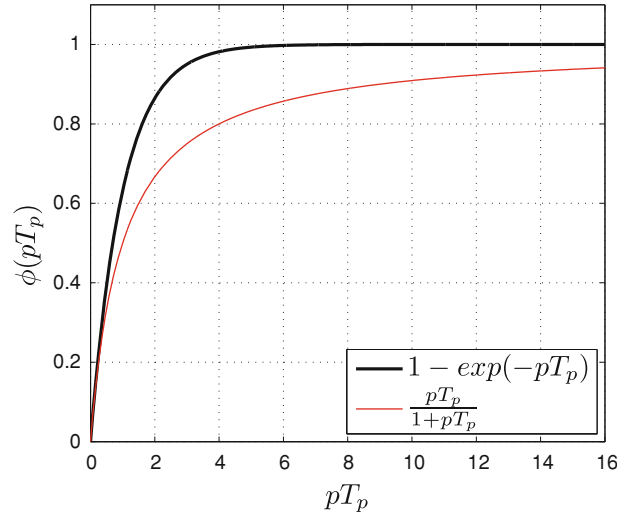


**Fig. 6** Physically acceptable expressions for the function  $\varphi(pT_p)$  appearing in Eq. (18)

$$\tan \alpha = \frac{a_p}{g} \varphi(pT_p), \quad \text{or} \quad \Pi_\alpha = \Pi_g \varphi(\Pi_\omega). \quad (18)$$

Now, while the expression of the function  $\varphi(pT_p)$  is unknown, physical argument indicates its limits as  $pT_p$  is very small or very large.

$$\lim_{pT_p \rightarrow 0} \varphi(pT_p) = 0 \quad \lim_{pT_p \rightarrow \infty} \varphi(pT_p) = 1 \quad (19)$$

large blocks or high-frequency pulses      small blocks or long-period pulses

With the two limiting values of  $\varphi(pT_p)$  established, one can propose approximate expressions for the function  $\varphi(pT_p)$ . For instance, the minimum allowable slenderness  $\alpha$  may be approximated with an exponential equation

$$\tan \alpha = \frac{a_p}{g} \left( 1 - e^{-\lambda pT_p} \right). \quad (20)$$

where  $\lambda$  is a coefficient that depends on the shape of the acceleration pulse. Figure 6 plots the function  $\varphi(pT_p) = 1 - \exp(-pT_p)$  as a function of  $pT_p$ . In the following subsection, we derive a mathematical expression of the function  $\varphi(pT_p)$  by using basic principles of dynamics.

## 5.2 Analytical approach

In order to address this problem analytically, we first examine what is the minimum initial angular velocity,  $\dot{\theta}(0)$ , that is needed to bring a free-standing block at the verge of overturning—a limit state that is defined when the diagonal of the block is vertical  $\theta(t_{ov}) = \alpha$  and the angular velocity at this position is zero ( $\dot{\theta}(t_{ov}) = 0$ ). At this limit state, for the angular velocity  $\dot{\theta}(t)$  to reach asymptotically the zero-value as  $\theta(t)$  tends to  $\alpha$ , it takes theoretically an infinite amount of time; therefore,  $t_{ov}$  is in any event sufficiently larger than any finite time interval which appears in the problem at hand. This sufficiently large time is illustrated in Fig. 7, which plots the rotation history of a  $2.5 \times 0.6$  m (left) and a  $7.5 \times 1.8$  m (right) free-standing block excited by a rectangular pulse with duration  $T_p = 0.5$  s and neighboring values of accelerations amplitudes that bring the rocking block closer and closer to its limit stability. In theory, the acceleration amplitude can be tuned to the extent that the block will take an infinite long time to decide whether it will re-center or overturn.

The minimum angular velocity needed to bring a free-standing block rocking on a rigid foundation at the verge of overturning is computed by equating the kinetic energy immediately after the initiation of motion,

$$T(t=0) = \frac{1}{2} I_o R^2 \dot{\theta}(0)^2 \quad (21)$$

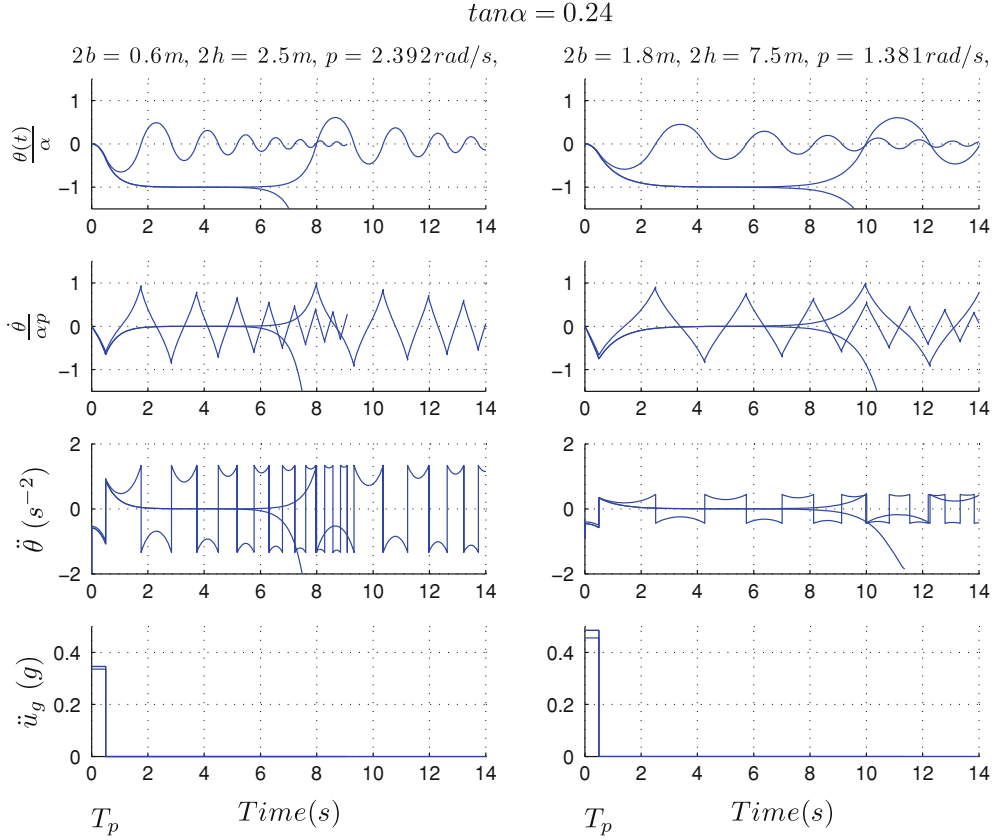


**Fig. 7** Rotations, angular velocities and angular accelerations of a  $2.5 \times 0.6\text{ m}$  (left) and a  $7.5 \times 1.8\text{ m}$  (right) block subjected to a 0.5 s long rectangular acceleration pulse that brings the block to its limit stability

with the potential energy at the verge of overturning ( $\theta(t = \text{large}) = \alpha$ ,  $\dot{\theta}(t = \text{large}) = 0$ )

$$V(t = \text{large}) = MgR(1 - \cos\alpha) \simeq \frac{\alpha^2}{2}MgR. \quad (22)$$

For rectangular blocks,  $I_o = (4/3)mR^2$ , and after equating the results from Eqs. (21) and (22), the minimum initial angular velocity needed to bring a rocking block ( $a$ ,  $p$ ) at the verge of overturning is

$$\dot{\theta}(0) = \alpha p. \quad (23)$$

Given the result of Eq. (23), our problem now reduces in identifying what shall be the acceleration amplitude and duration of a pulse capable of inducing an initial angular velocity  $\dot{\theta}(t = T_p) = \alpha p$ . It is known (Makris and Roussos [8, 10]) that the shape of the pulse influences the exact value of the slenderness needed for the block to remain standing; nevertheless, it is also known that the rectangular pulse has the strongest overturning potential among all other physically realizable pulses (differentiable acceleration signals that produce finite ground displacement) with the same amplitude and duration. Consequently, a rectangular pulse yields conservative results, which are attractive in design. Accordingly, we proceed by examining what is the angular velocity induced in a free-standing block excited by a rectangular pulse with acceleration amplitude  $a_p$  and duration  $T_p$ . Figure 2 (right) shows the free-body diagram of a free-standing block that is about to enter rocking motion due to a positive ground acceleration. With the system of axis shown, a positive acceleration will induce an initial negative rotation ( $\theta < 0$ ). Adopting the notation introduced by Shenton [6], let  $f_x > 0$  and  $f_z > 0$  be the horizontal and vertical reactions at the tip O' of the block. Dynamic equilibrium at this instant ( $\theta = 0$ ) gives

$$f_x(0) = m(a_p + h\ddot{\theta}(0)) \quad (24)$$

$$f_z(0) = m(g - b\ddot{\theta}(0)) \quad (25)$$

$$I_{cg}\ddot{\theta}(0) = -f_x(0)h + f_z(0)b \quad (26)$$

where  $I_{cg}$  is the moment of inertia of the block about its center of gravity (for rectangular blocks,  $I_{cg} = mR^2/3$ ). Substitution of Eqs. (24) and (25) into (26) gives the value of the angular acceleration  $\ddot{\theta}(0)$  at the instant when rocking initiates

$$\ddot{\theta}(0) = -p^2 \sin \alpha \left( \frac{a_p}{g \tan \alpha} - 1 \right). \quad (27)$$

Returning to Fig. 7, it is observed that the angular acceleration  $\ddot{\theta}(t)$  during the duration  $T_p$  of the rectangular acceleration pulse starts with a finite value, maintains a nearly constant value  $= \ddot{\theta}(0)$ , and subsequently increases by creating a small “corner area” until the motion reverses. The quantity of prime interest in this analysis is not the precise value of the angular acceleration  $\ddot{\theta}(t)$  within the interval  $0 < t < T_p$ ; but rather the area under the curve  $\ddot{\theta}(t)$  within this interval—that is the angular velocity  $\dot{\theta}(T_p)$ . Accordingly, the “corner area” that is created above the value  $\ddot{\theta}(0)$  is small compared with the overall area under the curve  $\ddot{\theta}(t)$  within the interval  $0 < t < T_p$ , thus the nearly linear increase in the angular velocity  $\dot{\theta}(t)$ ,  $0 < t < T_p$ .

Accordingly, at the expiration of the pulse, the angular velocity of the block is approximately

$$\dot{\theta}(t = T_p) = \int_0^{T_p} \ddot{\theta}(0) dt = -p^2 \sin \alpha \left( \frac{a_p}{g \tan \alpha} - 1 \right) \int_0^{T_p} dt \quad (28)$$

or

$$\dot{\theta}(t = T_p) = -p^2 \sin \alpha \left( \frac{a_p}{g \tan \alpha} - 1 \right) T_p \quad (29)$$

Consider now that the rectangular pulse  $\langle a_p, T_p \rangle$  is strong enough to bring the block at the verge of overturning [ $\theta(t = \text{large}) = \alpha$ ,  $\dot{\theta}(t = \text{large}) = 0$ ]. Given that the limit state at the verge of overturning happens after a very large time when compared with the duration of the pulse,  $T_p$  (see Fig. 7), the duration of the pulse can be assumed zero when compared with the time needed to reach the limit state. Accordingly, within the very large time scale of the limiting equilibrium, the angular velocity  $\dot{\theta}(t = T_p)$  given by (29) can be assumed as  $\dot{\theta}(t = 0)$ . With this consideration, and after dropping the minus sign in front of the right-hand side of (29)—which is merely associated with the direction of shaking—the equation of the right-hand sides of Eqs. (29) and (24) gives:

$$\alpha = p \sin \alpha \left( \frac{a_p}{g \tan \alpha} - 1 \right) T_p \quad (30)$$

For slender blocks,  $\alpha = \sin \alpha$  and Eq. (30) gives

$$\tan \alpha = \frac{a_p}{g} \frac{pT_p}{1 + pT_p} \quad (31)$$

Consequently, when a free-standing block with size  $R$  ( $p = \sqrt{\frac{3g}{4R}}$ ) is subjected to a rectangular acceleration pulse with amplitude  $a_p$  and duration  $T_p$ , the condition for the block to remain stable is  $\tan \alpha > \frac{a_p}{g} \frac{pT_p}{1 + pT_p}$ .

Equation (31) indicates that the minimum allowable slenderness  $\tan \alpha$  is equal to the acceleration that initiates uplifting,  $\frac{a_p}{g}$ , modified by the factor  $\frac{pT_p}{1 + pT_p}$ . For small blocks or long-period pulses (large  $pT_p$ ), the modification factor tends to unity and the static solution,  $a_p = \tan \alpha$  is recovered. For large blocks and more high-frequency pulses, the multiplication factor  $\frac{pT_p}{1 + pT_p}$  is smaller than unity, resulting in more slender configurations that can survive the same acceleration amplitude. Accordingly, in this sub-section the unknown function  $\varphi(pT_p)$  appearing in Eq. (18) was evaluated analytically using basic principles of dynamics. Figure 6

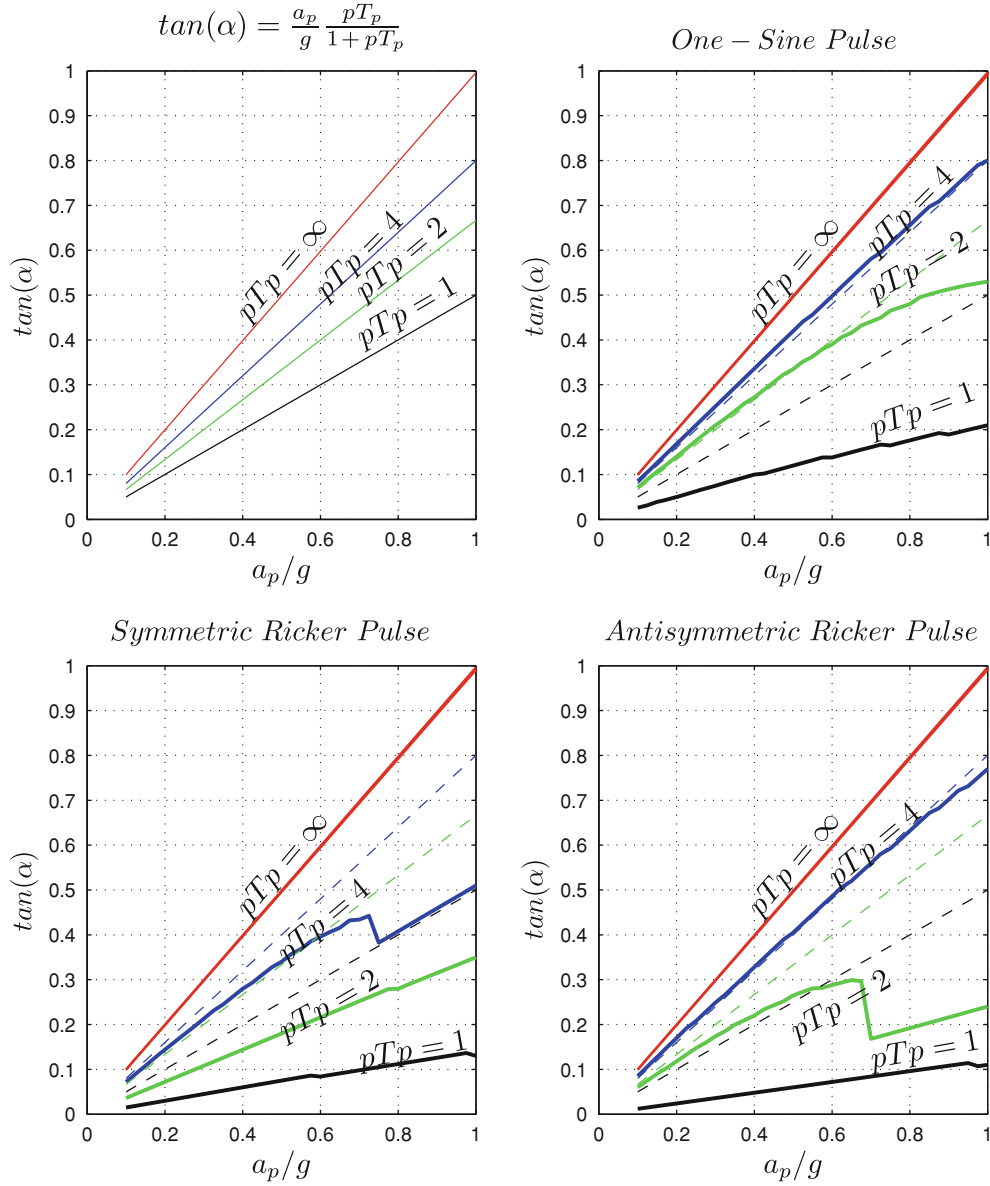


**Fig. 8** Top-left minimum design slenderness values. Other subplots: exact minimum slenderness values when the free-standing block is subjected to three popular acceleration pulses

plots the function  $\varphi(pT_p) = \frac{pT_p}{1+pT_p}$  next to the approximate expression  $\varphi(pT_p) = 1 - \exp(-pT_p)$  introduced earlier based solely on dimensional and physical arguments and shows that the modification factor  $\frac{pT_p}{1+pT_p}$  derived with the analytical approach offers a more slender configuration than the overconservative exponential function.

Figure 8 (top-left) plots the results of Eq. (31) for different values of  $pT_p$ . The other three subplots in Fig. 8 show the exact minimum stable slenderness values of free-standing blocks when subjected to a one-sine (top-right), a symmetric Ricker (bottom-left), and an antisymmetric Ricker (bottom-right) acceleration pulses as computed by solving numerically the nonlinear equation of motion given by Eq. (3). For all three physical realizable pulses (zero ground velocity at the expiration of the ground motion), the corresponding minimum allowable values for  $\tan \alpha$  are smaller than the conservative values that result from the rectangular pulse [top-left plot or Eq. (31)]. The only exception is the case of a one-sine pulse and  $pT_p = 4$  where the design slenderness is slightly lower than what is computed numerically. For this slight discrepancy ( $pT_p = 4$ ), it shall be recognized that for the size of columns that we are interested ( $p < 1.5$ ),  $T_p = \frac{4}{1.5} \approx 2.7$  is a rather

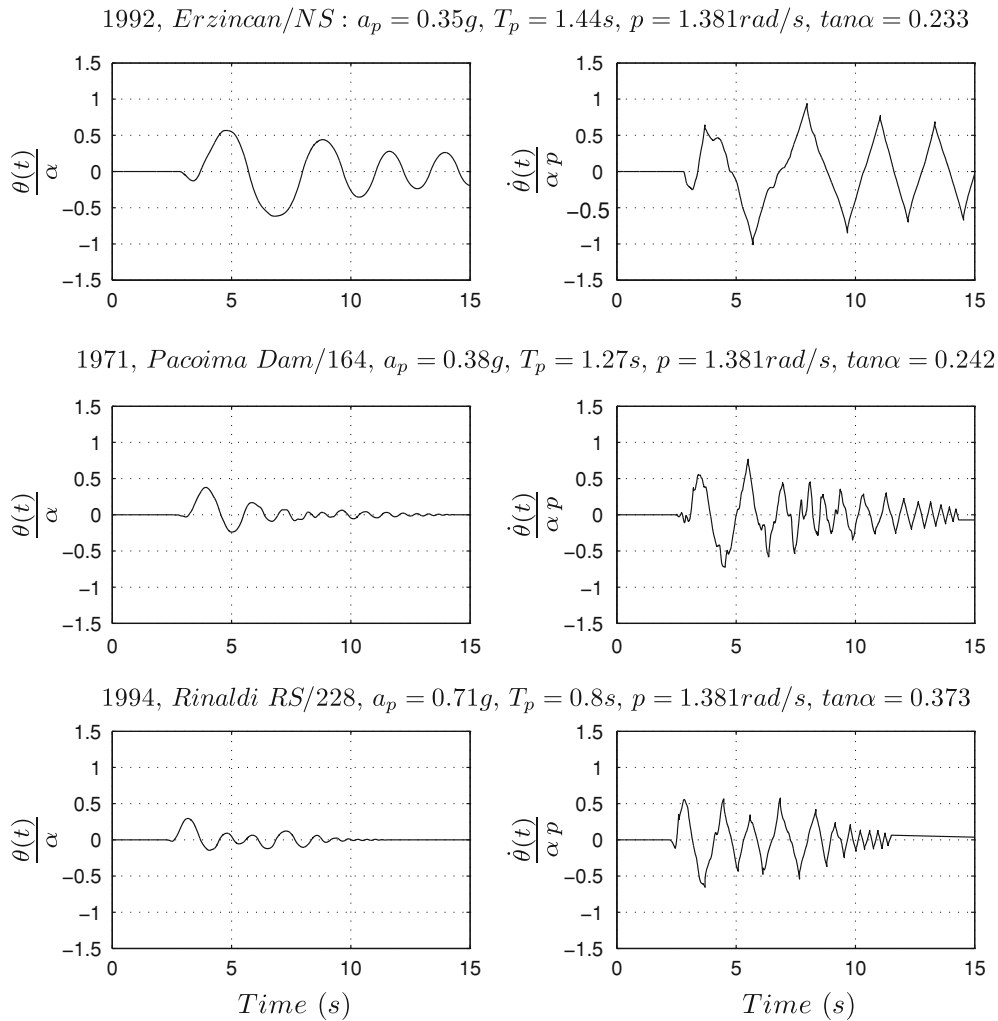


**Fig. 9** Response histories of 3 blocks with size  $p = 1.381$  rad/s and slenderness values as derived by Eq. (31) when excited by the three pulse-type recorded motions shown in Fig. 4

long pulse period. When such long pulse periods are expected, the minimum design slenderness offered by Eq. (31) shall be also confirmed with time-history analysis as shown in the examples offered below.

### 5.3 Validation of the design formula: examples

Figure 9 presents the rotational, and angular velocity histories of three blocks that have the same size  $p = 1.381$  rad/sec (the size of the columns of the Temple of Apollo in Corinth) and values of slenderness as derived from Eq. (31) in which the values of  $a_p$  and  $T_p$  are those of the corresponding distinguishable pulses shown in Fig. 4. The response histories shown in Fig. 9 show that the design slenderness as offered by Eq. (31) is sufficient to ensure stability of the blocks with size  $p = 1.381$  rad/s. It is worth mentioning that the peak rotations are kept at or below  $\alpha/2$  for all three strong records, showing that the proposed design slenderness is dependable.

## 6 Application of the design expression

In several occasions, tall slender free-standing structures challenge the intuition of the observer regarding their seismic stability through time. As an example, Fig. 10 shows a view of the Temple of Apollo in Corinth where



**Fig. 10** View of the temple of Apollo, Corinth. Its monolithic, free-standing columns remain standing in an area of high seismicity since 540BC

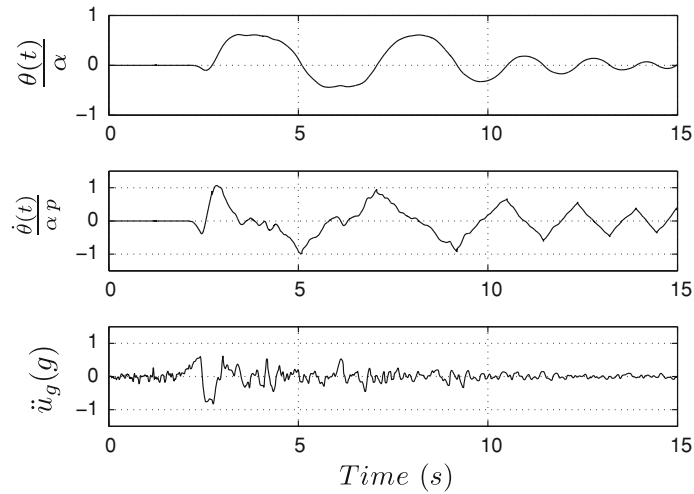


**Fig. 11** Rotation and angular velocity time histories of the column of the Temple of Apollo in Corinth ( $p = 1.281$  rad/s,  $\tan \alpha = 0.24$ ) when excited by the 1994 Rinaldi Station/228 record

its  $7.5 \times 1.8$  m monolithic columns remain standing from the ancient times in an area with high seismicity since 540BC.

The free-standing columns have a slenderness value  $\tan \alpha = 1.8/7.5 = 0.24$  and a frequency parameter  $p = 1.381$ . The sufficiency of the slenderness of these columns is checked against the OTE ground motion recorded during the 1995 Aegion earthquake. This is one of the strongest ground motions ever recorded in Greece with a coherent long-period pulse with duration  $T_p = 0.5$  s and an acceleration amplitude  $a_p = 0.5$  g. This coherent pulse resembles a symmetric Ricker wavelet [29]; nevertheless, in order to be on the conservative side, we assume that these are the characteristics of a rectangular acceleration pulse. Despite this enhancement regarding the overturning potential of the excitation pulse, Eq. (31) yields a minimum slenderness value,  $\tan \alpha = 0.5 \times 0.5 / (1 + 0.5) = 0.166$ —a value that is appreciably less than the actual slenderness value of the column,  $\tan \alpha = 0.24$ . This elementary hand calculation made possible with the use of Eq. (31) (which accounts in a conservative manner for the enhanced dynamic stability of free-standing rocking objects) explains the ample seismic stability of the emblematic free-standing columns built during the ancient times.

Equation (31) (see also Fig. 9) indicates that for the 1992 Erzincan record, the minimum design slenderness of the columns to survive the ground shaking is  $\tan(\alpha) = 0.233$ , whereas for the 1971 Pacoima Dam Record,  $\tan(\alpha) = 0.242$ . One of these values is less, and the other is equal to the slenderness of the columns of the Temple of Apollo in Corinth:  $\tan(\alpha) = 0.24$ . Therefore; the columns of the Temple of Apollo survive these two aforementioned strong records.

The Rinaldi Station Record 228 shown at the bottom of Fig. 4 is an unusually strong record having a distinguishable pulse with  $a_p = 0.71$  g and  $T_p = 0.8$  s. Equation (31) yields that for these pulse characteristics

( $a_p = 0.71g$  and  $T_p = 0.8s$ ) and the size of the column of the Temple of Apollo ( $p = 1.381$  rad/sec), the minimum design slenderness of the column is  $\tan(\alpha) = 0.373$ —a slenderness value that is appreciably larger than the  $\tan(\alpha) = 0.24$  value of the columns of temple of Apollo in Corinth. Figure 11 shows the rotation and angular velocity histories of the columns of Temple of Apollo in Corinth ( $p = 1.381$  rad/sec,  $\tan(\alpha) = 0.24$ ) when excited by the 1994 Rinaldi Station Record 228. Despite its smaller slenderness than the minimum design value ( $\tan(\alpha) = 0.24 < 0.373$ ), the column does not overturn, showing that Eq. (31) offers a conservative value for the design slenderness of large blocks than are allowed to rock.

## 7 Conclusions

In this paper, we examined the problem of sizing the width of tall, free-standing structures which are intended to rock, yet shall remain stable during the maximum expected earthquake shaking.

The paper first introduces the concept of acceleration pulses such as the one-sine pulse, the symmetric Ricker wavelet, and the antisymmetric Ricker wavelet and indicates that such pulses can characterize the destructive coherent component of several near-source ground motions. Subsequently, the paper presents the dimensionless products that govern the dynamic response of a free-standing block and by using basic principles of dynamics derives a close form expression that offers the minimum design slenderness that is sufficient for a free-standing block with a given size to survive a pulse-like motion with known acceleration intensity and duration.

**Acknowledgments** Partial financial support for this study has been provided to the second author by the Alexander S. Onassis Public Benefit Foundation and by the EU research project “DARE” (“Soil-Foundation-Structure Systems Beyond Conventional Seismic Failure Thresholds: Application to New or Existing Structures and Monuments”), which is funded through the 7th Framework Program “Ideas”, Support for Frontier Research—Advanced Grant, under contract number ERC-2—9-AdG 228254-DARE to professor G. Gazetas.

## References

1. Milne, J.: Seismic experiments. *Trans. Seismol. Soc. Jpn.* **8**, 1–82 (1885)
2. Housner, G.W.: The behaviour of inverted pendulum structures during earthquakes. *Bull. Seismol. Soc. Am.* **53**(2), 404–417 (1963)
3. Yim, S.C.S., Chopra, A.K., Penzien, J.: Rocking response of rigid blocks to earthquakes. *Earthq. Eng. Struct. Dyn.* **8**(6), 565–587 (1980)
4. Spanos, P.D., Koh, A.S.: Rocking of rigid blocks due to harmonic shaking. *J. Eng. Mech. ASCE* **110**(11), 1627–1642 (1984)
5. Hogan, S.J.: On the dynamics of rigid-block motion under harmonic forcing. *Proc., Royal Soc., London*, A425, pp. 441–476 (1989)
6. Shenton, H.W. III.: Criteria for initiation of slide, rock, and slide-rock rigid-body modes. *J. Eng. Mech. ASCE* **122**(7), 690–693 (1996)
7. Shi, B., Anooshehpour, A., Zeng, Y., Brune, J.N.: Rocking and overturning of precariously balanced rocks by earthquake. *Bull. Seismol. Soc. Am.* **86**(5), 1364–1371 (1996)
8. Makris, N., Roussos, Y.: Rocking response of rigid blocks under near-source ground motions. *Geotech. Lond.* **50**(3), 243–262 (2000)
9. Zhang, J., Makris, N.: Rocking response of free-standing blocks under cycloidal pulses. *J. Eng. Mech. (ASCE)* **127**(5), 473–483 (2001)
10. Makris, N., Roussos, Y.: Rocking response and overturning of equipment under horizontal pulse-type motions. Rep. No. PEER-98/05, Pacific Earthquake Engrg. Res. Ctr., University of California, Berkeley, California (1998)
11. Aslam, M., Scalise, D.T., Godden, W.G.: Earthquake rocking response of rigid bodies. *J. Struct. Div. ASCE* **106**(2), 377–392 (1980)
12. Tso, W.K., Wong, C.M.: Steady state rocking response of rigid blocks Part 1: analysis. *Earthq. Eng. Struct. Dyn.* **18**(1), 89–106 (1989)
13. Tso, W.K., Wong, C.M.: Steady state rocking response of rigid blocks Part 2: experiment. *Earthq. Eng. Struct. Dyn.* **18**(1), 107–120 (1989)
14. Psycharis, I.N.: Dynamic behaviour of rocking two-block assemblies. *Earthq. Eng. Struct. Dyn.* **19**, 555–575 (1990)
15. Makris, N., Konstantinidis, D.: The rocking spectrum and the limitations of practical design methodologies. *Earthq. Eng. Struct. Dyn.* **32**, 265–289 (2003)
16. Apostolou, M., Gazetas, G., Garini, E.: Seismic response of slender rigid structures with foundation uplifting. *Soil Dyn. Earthq. Eng.* **27**(7), 642–654 (2007)
17. Anastasopoulos, I., Gazetas, G., Loli, M., Apostolou, M., Gerolymos, N.: Soil failure can be used for earthquake protection of structures. *Bull. Earthq. Eng.* **8**(2), 309–326 (2010)
18. Beck, J.L., Skinner, R.I.: The seismic response of a reinforced concrete bridge pier designed to step. *Earthq. Eng. Struct. Dyn.* **2**, 343–358 (1973). doi:[10.1002/eqe.4290020405](https://doi.org/10.1002/eqe.4290020405)

19. Pecker, A.: Design and construction of the foundations of the Rion Antirion Bridge. In: Proceedings of the 1st Greece–Japan Workshop on Seismic Design, Observation, Retrofit of Foundations, Athens, pp. 119–130 (2005)
20. Yashinsky, M., Karshenas, M.J.: Fundamentals of Seismic Protection for Bridges. Earthquake Engineering Research Institute, Oakland (2003)
21. Gelagoti, F., et al.: Rocking-isolated frame structures: Margins of safety against toppling collapse and simplified design approach. *Soil Dyn. Earthq. Eng.* (2011). doi:[10.1016/j.soildyn.2011.08.008](https://doi.org/10.1016/j.soildyn.2011.08.008)
22. Bertero, V.V., Mahin, S.A., Herrera, R.A.: Aseismic design implications of near-fault San Fernando earthquake records. *Earthq. Eng. Struct. Dyn.* **6**, 31–42 (1978)
23. Campillo, M., Gariel, J.C., Aki, K., Sanchez-Sesma, F.J.: Destructive strong ground motion in Mexico City: source, path and site effects during the great 1985 Michoagan earthquake. *Bull. Seismol. Soc. Am.* **79**(6), 1718–1735 (1989)
24. Iwan, W.D., Chen, X.D.: Important near-field ground motions data from the Landers earthquake. In: Proceedings 10th European Conference on Earthquake Engineering, pp. 229–234, Vienna, Austria (1994)
25. Hall, J.F., Heaton, T.H., Halling, M.W., Wald, D.J.: Near-source ground motion and its effects on flexible buildings. *Earthq. Spectr.* **11**(4), 569–605 (1995)
26. Heaton, T.H., Hall, J.F., Wald, D.J., Halling, M.W.: Response of high-rise and base-isolated buildings to a hypothetical Mw 7.0 blind thrust earthquake. *Science* **267**, 206–211 (1995)
27. Makris, N.: Rigidity–plasticity–viscosity: can electrorheological dampers protect base-isolated structures from near-source ground motions?. *Earthq. Eng. Struct. Dyn.* **26**, 571–591 (1997)
28. Mavroeidis, G.P., Papageorgiou, A.S.: A mathematical representation of near-fault ground motions. *Bull. Seismol. Soc. Am.* **93**(3), 1099–1131 (2003)
29. Vassiliou, M.F., Makris, N.: Estimating time scales and length scales in pulslike earthquake acceleration records with wavelet analysis. *Bull. Seismol. Soc. Am.* **101**(2), 596–618 (2011)
30. Vassiliou, M.F., Makris, N.: Analysis of the rocking response of rigid blocks standing free on a seismic isolated base. *Earthq. Eng. Struct. Dyn.* (2011) (published online). doi:[10.1002/eqe.1124](https://doi.org/10.1002/eqe.1124)
31. Veletsos, A.S., Newmark, N.M., Chelepati, C.V.: Deformation spectra for elastic and elastoplastic systems subjected to ground shock and earthquake motions. In: Proceedings of the 3rd World Conference on Earthquake Engineering, vol. II, pp. 663–682, Wellington, New Zealand (1965)
32. Makris, N., Chang, S.-P.: Effect of viscous, viscoplastic and friction damping on the response of seismic isolated structures. *Earthq. Eng. Struct. Dyn.* **29**(1), 85–107 (2000)
33. Alavi, B., Krawinkler, H.: Effects of near-source ground motions on frame-structures. Technical Report No. 138, The John A. Blume Earthquake Engineering Center, Stanford University (2001)
34. Aki, K., Bouchon, M., Chouet, B., Das, S.: Quantitative prediction of strong motion for a potential earthquake fault. *Annali di Geofisica* **30**, 341–368 (1977)
35. Brune, J.N.: Tectonic stress and the spectra of seismic shear waves from earthquakes. *J. Geophys. Res.* **75**, 4997–5009 (1970)
36. Aki, K.: Strong-motion seismology. In earthquakes: observation, theory and interpretation. In: Kanamori, H., Boschi, E. (eds.) Proceedings of the International School of Physics, Enrico Fermi, Course 85. North-Holland, Amsterdam, pp. 223–250 (1983)
37. Makris, N., Black, C.J.: Dimensional analysis of rigid-plastic and elastoplastic structures under pulse-type excitations. *J. Eng. Mech. (ASCE)* **130**(9), 1006–1018 (2004)
38. Makris, N., Black, C.J.: Dimensional analysis of bilinear oscillators under pulse-type excitations. *J. Eng. Mech. (ASCE)* **130**(9), 1019–1031 (2004)
39. Karavasilis, T.L., Makris, N., Bazeos, N., Beskos, D.E.: Dimensional response analysis of multistory regular steel MRF subjected to pulslike earthquake ground motions. *J. Struct. Eng.* **136**, 921–932 (2010)
40. Ricker, N.: Further developments in the wavelet theory of seismogram structure. *Bull. Seismol. Soc. Am.* **33**, 197–228 (1943)
41. Ricker, N.: Wavelet functions and their polynomials. *Geophysics* **9**, 314–323 (1944)
42. Addison, P.: The Illustrated Wavelet Transform Handbook: Introductory Theory and Applications in Science, Engineering, Medicine and Finance. Institute of Physics, London (2002)
43. MATLAB: High-performance Language of Technical Computing. The Mathworks, Inc., Natick, MA (2002)